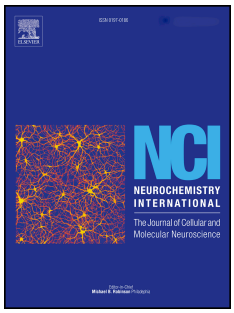

Analysis of Reelin signaling and neurodevelopmental trajectory in primary cultured cortical neurons with *RELN* deletion identified in schizophrenia

Yumi Tsuneura, Masahito Sawahata, Norimichi Itoh, Ryoya Miyajima, Daisuke Mori, Takao Kohno, Mitsuharu Hattori, Akira Sobue, Taku Nagai, Hiroyuki Mizoguchi, Toshitaka Nabeshima, Norio Ozaki, Kiyofumi Yamada

PII: S0197-0186(20)30345-4

DOI: https://doi.org/10.1016/j.neuint.2020.104954

Reference: NCI 104954

To appear in: *Neurochemistry International*

Received Date: 23 November 2020

Revised Date: 20 December 2020

Accepted Date: 27 December 2020

Please cite this article as: Tsuneura, Y., Sawahata, M., Itoh, N., Miyajima, R., Mori, D., Kohno, T., Hattori, M., Sobue, A., Nagai, T., Mizoguchi, H., Nabeshima, T., Ozaki, N., Yamada, K., Analysis of Reelin signaling and neurodevelopmental trajectory in primary cultured cortical neurons with *RELN* deletion identified in schizophrenia , *Neurochemistry International*, https://doi.org/10.1016/j.neuint.2020.104954.

CRediT authorship contribution statement:

Yumi Tsuneura: Data curation, Formal analysis, Investigation, Writing – original draft

Masahito Sawahata: Investigation, Resources

Norimichi Itoh: Investigation, Resources

Ryoya Miyajima: Formal analysis, Investigation

Daisuke Mori: Resources, Methodology

Takao Kohno: Resources, Writing – review & editing

Mitsuharu Hattori: Resources, Writing – review & editing

Akira Sobue: Writing – review & editing

Taku Nagai: Writing – review & editing

Hiroyuki Mizoguchi: Writing – review & editing

Toshitaka Nabeshima: Supervision, Writing – review & editing

Norio Ozaki: Conceptualization, Resources

Kiyofumi Yamada: Conceptualization, Supervision, Funding acquisition, Project administration, Writing – review & editing

CRediT authorship contribution statement:

Yumi Tsuneura: Data curation, Formal analysis, Investigation, Writing – original draft

Masahito Sawahata: Investigation, Resources

Norimichi Itoh: Investigation, Resources

Ryoya Miyajima: Formal analysis, Investigation

Daisuke Mori: Resources, Methodology

Takao Kohno: Resources, Writing – review & editing

Mitsuharu Hattori: Resources, Writing – review & editing

Akira Sobue: Writing – review & editing

Taku Nagai: Writing – review & editing

Hiroyuki Mizoguchi: Writing – review & editing

Toshitaka Nabeshima: Supervision, Writing – review & editing

Norio Ozaki: Conceptualization, Resources

Kiyofumi Yamada: Conceptualization, Supervision, Funding acquisition, Project administration, Writing – review & editing

Analysis of Reelin signaling and neurodevelopmental trajectory in primary cultured cortical neurons with *RELN* deletion identified in schizophrenia

Yumi Tsuneura[a], Masahito Sawahata[a], Norimichi Itoh[a], Ryoya Miyajima[a], Daisuke Mori[b,c], Takao Kohno[d], Mitsuharu Hattori[d], Akira Sobue[e], Taku Nagai[f], Hiroyuki Mizoguchi[a], Toshitaka Nabeshima[g], Norio Ozaki[b], Kiyofumi Yamada[a,*]

[a]Department of Neuropsychopharmacology and Hospital Pharmacy, Nagoya University, Graduate School of Medicine, Nagoya, Aichi, Japan; [b]Department of Psychiatry, Nagoya University Graduate School of Medicine, Nagoya, Aichi, Japan; [c]Brain and Mind Research Center, Nagoya University, Nagoya, Aichi, Japan; [d]Department of Biomedical Science, Graduate School of Pharmaceutical Sciences, Nagoya City University, Nagoya, Aichi, Japan; [e]Department of Neuroscience and Pathobiology, Research Institute of Environmental Medicine, Nagoya University, Nagoya, Aichi, Japan; [f]Division of Behavioral Neuropharmacology, Project Office for Neuropsychological Research Center, Fujita Health University, Toyoake, Aichi, Japan; [g]Advanced Diagnostic System Research Laboratory, Graduate School of Health Sciences, Fujita Health University, Toyoake, Aichi, Japan.

*Corresponding author: kyamada@med.nagoya-u.ac.jp

Department of Neuropsychopharmacology and Hospital Pharmacy, Nagoya University, Graduate School of Medicine, Nagoya, Aichi, Japan

Abstract

Reelin, an extracellular matrix protein, is secreted by Cajal-Retzius cells and plays crucial roles in the development of brain structures and neuronal functions. Reductions in Reelin cause the brain dysfunctions associated with mental disorders, such as schizophrenia. A recent genome-wide copy number variation analysis of Japanese schizophrenia patients identified a novel deletion in *RELN* encoding Reelin. To clarify the pathophysiological role of the *RELN* deletion, we developed transgenic mice carrying the *RELN* deletion (*Reln*-del) and found abnormalities in their brain structures and social behavior. In the present study, we performed an *in vitro* analysis of Reelin expression, intracellular Reelin signaling, and the morphology of primary cultured cortical neurons from wild-type (WT) and *Reln*-del mice. Reelin protein levels were lower in *Reln*-del neurons than in WT neurons. Dab1 expression levels were significantly higher in *Reln*-del neurons than in WT neurons, suggesting that Reelin signaling was decreased in *Reln*-del neurons. Reelin was mainly expressed in γ-aminobutyric acid (GABA)-ergic inhibitory neurons, but not in parvalbumin (PV)-positive neurons. A small proportion of Ca^{2+}/calmodulin-dependent protein kinase II α subunit (CaMKIIα)-positive excitatory neurons also expressed Reelin. In comparisons with WT neurons, significant decreases were observed in neurite lengths and branch points as well as in the number of postsynaptic density protein 95 (PSD95) immunoreactive puncta in *Reln*-del neurons. A disintegrin and metalloproteinase with thrombospondin motifs-3 (ADAMTS-3) is a protease that inactivates Reelin by cleavage at the N-t site. The knockdown of ADAMTS-3 by short hairpin RNAs suppressed Reelin cleavage in conditioned medium and reduced Dab1 expression, indicating that Reelin signaling was enhanced in the primary

cultured cortical neurons of WT and heterozygous *Reln*-del. Accordingly, the inhibition of ADAMTS-3 may be a potential candidate in the clinical treatment of schizophrenia by enhancing Reelin signaling in the brain.

Keywords

Reelin, Schizophrenia, Cortex, Neuron, Dab1, ADAMTS-3

1. Introduction

Reelin is a large secreted protein that is necessary for the development of brain structures and function. In the developing brain, Reelin is mainly expressed in Cajal-Retzius cells that are present on the surface of the neocortex (Meyer et al., 1999), and Reelin regulates neuronal migration (Hartfuss et al., 2003) and the formation of proper cortical layers (Curran and D'Arcangelo, 1998). In the adult brain, Reelin is primarily expressed in γ-aminobutyric acid (GABA)-ergic neurons (Pesold et al., 1999). Secreted Reelin stimulates Src family tyrosine kinases (SFKs) and promotes the tyrosine phosphorylation of intracellular Dab1 (Bock and Herz, 2003) through binding to very low density lipoprotein receptor (VLDLR) and apolipoprotein E receptor 2 (ApoER2) (Benhayon et al., 2003). Phosphorylated Dab1 activates the downstream pathway, leading to the development of synaptic plasticity (Weeber et al., 2002), neurite growth (Niu et al., 2004), dendritic spines (Niu et al., 2008), and neuronal migration (Tissir and Goffinet, 2003).

Previous studies suggested that decreases in Reelin expression were associated with neuropsychiatric disorders, such as schizophrenia, autism, and Alzheimer's disease (Wasser and Herz, 2017). Reelin protein and

mRNA expression levels were lower in schizophrenia patients than in non-psychiatric patients (Impagnatiello et al., 1998). A recent genome-wide copy number variation (CNV) analysis of Japanese schizophrenia patients identified a novel deletion in *RELN* encoding Reelin (Kushima et al., 2017). A male patient with the exonic deletion of *RELN* exhibited positive and negative symptoms with cognitive impairment, and the amount of Reelin was decreased in his serum (Sobue et al., 2018). We developed genetically modified mice that mimic the *RELN* deletion of the Japanese schizophrenia patient (*Reln*-del). The cerebellum of homozygous *Reln*-del mice (*Reln*-del$^{-/-}$) was markedly atrophied and cortical layers were abnormal. Heterozygous *Reln*-del mice (*Reln*-del$^{+/-}$) showed several abnormalities in seeking behavior for social novelty (Sawahata et al., 2020). However, the mechanisms underlying the behavioral abnormalities and neuronal characteristics of *Reln*-del mice have not yet been elucidated.

Reelin supplementation improves neuronal function *in vivo* and *in vitro*. A microinjection of the Reelin protein into the brain enhanced learning and memory, synaptic plasticity, and dendritic spine density in adult wild-type (WT) mice (Rogers et al., 2011), and improved deficits in associative learning and memory function as well as pre-pulse inhibition in *Reeler* mice with a 50% reduction in Reelin expression (Rogers et al., 2013). Maternal immune activation (MIA), a schizophrenia animal model induced by the administration of polyinosinic: polycytidylic acid (poly I:C) during pregnancy, showed impaired recognition and increased anxiety-like behaviors, and an injection of Reelin into the hippocampus ameliorated these behavioral abnormalities (Ibi et al., 2020). Reelin supplementation to cultured hippocampal neurons increased dendritic spine density (Kim et al., 2015). Reelin also enhanced glutamic acid-induced calcium influx to activate the NMDA receptor function of primary cortical neurons (Chen et al., 2005). Furthermore, the dendrite length and branch number of cultured hippocampal

neurons were significantly increased in Reelin-containing medium (Niu et al., 2004). Collectively, these findings indicate that neural deficits and brain dysfunctions associated with reductions in Reelin expression were ameliorated by the supplementation of Reelin into the brain.

Endogenous Reelin is mainly inactivated by a disintegrin and metalloproteinase with thrombospondin motifs-3 (ADAMTS-3). ADAMTS-3 is an enzyme that specifically cleaves Reelin between Pro1243 and Ala1244, called the N-t site (Koie et al., 2014). Reelin degradation was markedly suppressed in the brains of conditional knockout (cKO) mice of ADAMTS-3, whereas the levels of active Reelin, which is capable of receptor binding, were elevated (Ogino et al., 2017). Furthermore, the number and length of dendritic branches were increased in the ADAMTS-3 cKO mice (Ogino et al., 2017). Therefore, the inhibition of ADAMTS-3 activity in the brains of patients with neuropsychiatric disorders, such as schizophrenia, may enhance Reelin signaling, leading to improvements in neuronal morphology and function, and, thus, clinical symptoms. However, since no inhibitors specific for ADAMTS-3 have been identified, ADAMTS-3 needs to be continuously inhibited using a new approach to test this hypothesis.

In the present study, we generated a primary culture of cortical neurons from *Reln*-del mice to characterize *Reln*-del neurons as a new schizophrenia model *in vitro*. We found that Reelin production and intracellular signaling were decreased in *Reln*-del neurons. In addition, *Reln*-del neurons exhibited some deficits in neurite development and synapse formation. The present results also demonstrated that the ADAMTS-3 knockdown method by short hairpin RNAs (shRNAs) suppressed secreted Reelin degradation in WT and *Reln*-del neurons.

2. Materials and methods

2.1. Animals

C57BL/6J mice were obtained from Japan SLC Inc. (Hamamatsu, Japan). *Reln*-del mice were generated in a C57BL/6J genetic background as described previously (Sawahata et al., 2020). WT littermates were used as controls. All animal experiments in the present study were approved by the Animal Care and Use Committee of Nagoya University, and complied with the Principles for the Care and Use of Laboratory Animals by the Japanese Pharmacological Society and the National Institutes of Health Guide for the Care and Use of Laboratory Animals.

2.2. Plasmid construction

ADAMTS-3 knockdown experiments were performed using shRNAs expressing a lentiviral system as reported previously (Tsujimura et al., 2015). To elucidate the shRNA sequences for the ADAMTS-3 knockdown, lentivirus plasmids, including candidate ADAMTS-3 shRNA (shRNA#1-5) and control shRNA (non-target) inserted into the pLKO.1-puro vector, were prepared from MISSION® shRNA Bacterial Glycerol Stock (Sigma-Aldrich, St. Louis, MO, USA). The target sequences for shRNA are listed in Supplementary Fig. 2.

To investigate the effects of the ADAMTS-3 knockdown on primary cultured cortical neurons from WT and *Reln*-del$^{+/-}$mice, the target sequences for shRNAs were as follows: shControl as a negative control: 5’-CAACAAGATGAAGAGCACCAA-3’ (Schramek et al., 2014), shADAMTS-3: 5’-GTGTCATCTAACTCAGAGCAT-3’ (the same sequence as shRNA#2 in Supplementary Fig. 2). These

sequences were inserted into the shRNA and EGFP expression vector (pLLX), which was generously provided by Drs. Z. Zhou and Greenberg, M. E (Lois et al., 2002; Zhou et al., 2006).

2.3. Lentivirus production

HEK293T cells were plated on 100-mm culture dishes (Corning, Corning, NY, USA) and cultured in DMEM (Sigma-Aldrich) containing 10% FBS (Gibco, Carlsbad, CA, USA), 100 units/mL of penicillin, 0.1 mg/mL of streptomycin, and 0.25 μg/mL of amphotericin B (Nacalai, Kyoto, Japan) under humidified air containing 5% CO_2 at 37°C. HEK293T cells were transfected with shRNA plasmid DNA, the envelope plasmid, and packaging plasmid in Opti-MEM medium (Gibco) and PEI MAX - transfection grade linear polyethylenimine hydrochloride (MW 40,000) (Polysciences, Inc., Warrington, FL, USA). Transfected HEK293T cells were incubated at 37°C overnight, and the medium was replaced with fresh culture medium the next day. Twenty-four hours after medium replacement, the virus-containing supernatant was collected and centrifuged at 3,000 × *g* for 10 min followed by 6,000 × *g* overnight. The pellet containing the lentivirus was suspended in 200 μL of DPBS (Gibco). Regarding the copy number quantification of the lentivirus, total RNA was purified by QIAamp Viral RNA mini (QIAGEN, Hilden, Germany). RNA concentrations were measured using the NanoDrop 2000c spectrophotometer (Thermo, Waltham, MA, USA). cDNA was synthesized from purified total RNA using the Superscript III First-Strand Synthesis SuperMix for qRT-PCR (Invitrogen, Eugene, OR, USA). Quantitative real-time reverse transcription (qRT)-PCR was performed using the 7300 Real-time PCR System (Applied Biosystems, Foster City, CA, USA) in 25 μL of reaction mixture containing 12.5 μL of the Power SYBR Green PCR Master Mix (Applied Biosystems), 1

μL of cDNA, and 0.5 μM of primers. Data were analyzed using a standard curve prepared based on pLLX containing EGFP. Data were analyzed using the $2^{-\Delta\Delta CT}$ method. The primers used in the present study were as follows: EGFP forward, 5'-CGTAAACGGCCACAAGTTCA-3', EGFP reverse, 5'-CTTCATGTGGTCGGGGTAGC-3'.

2.4. Preparation of primary cultured cortical neurons and lentivirus infection

Reln-del$^{+/-}$ male mice and *Reln*-del$^{+/-}$ female mice were crossed to generate WT, *Reln*-del$^{+/-}$, and *Reln*-del$^{-/-}$ mice. Cortical neurons were prepared from the cortices of embryonic day (E) 15. Cortical tissues were incubated in Hanks' balanced salt solution (Gibco) with 0.25% trypsin (Gibco) and 0.01% DNase (Roche Diagnostics GmbH, Mannheim, Germany) at 37°C for 10 min. The cortices were washed with Neurobasal medium (Gibco), followed by trituration with an electric pipettor and micropipette. Cells were then plated at 600,000 cells/well in poly-D-lysine-coated 6-well plates (IWAKI) for total RNA and protein extraction, including ADAMTS-3 knockdown experiments. In the immunocytochemical assay, cells were plated at 10,000 cells/well on 15-mm coverslips (Matsunami, Kishiwada, Japan) on 12-well plates (Corning) coated with poly-D-lysine (Gibco). Regarding live imaging, cells were plated at 10,000 cells/well on 12-well plates (Corning) coated with poly-D-lysine (Gibco). Cultured neurons were incubated in Neurobasal medium containing 10% FBS under humidified air containing 5% CO_2 at 37°C. After 3 h, the medium was replaced with Neurobasal medium containing B-27 supplement (Gibco) and 0.5 mM GlutaMax-I (Gibco). Half of the conditioned medium was replaced with fresh medium every 3 or 4 days. In the ADAMTS-3 knockdown experiment, primary cultured

cortical neurons were transfected with the lentivirus (10^8 copies/well) at 10 days *in vitro* (DIV10) and collected at DIV20. Genotyping was performed as previously described (Sawahata et al., 2020).

2.5. Analysis of ADAMTS-3 knockdown efficiency

Total RNA was extracted at DIV20 by the RNeasy Mini Kit (Qiagen) from cultured cortical neurons transfected with the lentivirus and qRT-PCR was performed as described in 2.3. Lentivirus production. Data were analyzed using the $2^{-\Delta\Delta CT}$ method. Glyceraldehyde-3-phosphate dehydrogenase (GAPDH) was used as an internal control. The primers used in the present study were as follows: ADAMTS-3 forward, 5'-CAGGTTCTGTGCAGGACTGG-3', ADAMTS-3 reverse, 5'-GGTATGGAGCAGTATCTTGC-3', ADAMTS-2 forward, 5'-GGCCTGATCCTGACTCACCT-3', ADAMTS-2 reverse, 5'-CCTCCGTCCTCTGTGTTGCT-3', GAPDH forward, 5'-CAATGTGTCCGTCGTGGATCT-3', GAPDH reverse, 5'-GTCCTCAGTCTAGCCCAAGATG-3'.

2.6. Reelin mRNA expression analysis

Medial prefrontal cortex (mPFC) tissue was obtained from WT and *Reln*-del$^{+/-}$ adult male mice (8-17 weeks old). Total RNA extraction and qRT-PCR were performed as described in 2.3 Lentivirus production. Reelin mRNA expression levels were examined using the primer sets for the conserved region and deleted region in *Reln*-del (Supplementary Fig. 1). GAPDH mRNA was used as an internal control and measured using the same primers in 2.5. Analysis of ADAMTS-3 knockdown efficiency. The primers for Reelin mRNA were as follows:

Reelin forward (conserved region), 5'-AGCACCTTCTTTGATGGCTTGCTGG-3', Reelin reverse (conserved region), 5'-CCACACTGCACATAAACTGGTTACC-3', Reelin forward (deleted region), 5'-CCCAGCCCAGACAGACAGTT -3', Reelin reverse (deleted region), 5'-CCAGGTGATGCCATTGTTGA-3'.

2.7. Western blotting (WB)

Regarding WB of intracellular Reelin and Dab1, proteins were extracted from cultured cortical neurons at DIV20 with 200 μL of sodium dodecyl sulfate (SDS) sample buffer (62.5 mM Tris-HCl (pH 6.8), 2% SDS, 10% glycerol, 0.01% bromophenol blue, and 5% 2-mercaptoethanol). The lysate was heated at 99°C for 10 min for the analysis of Dab1 expression, but not Reelin to prevent aggregation. Ten microliters of protein samples were loaded onto the 10% SDS polyacrylamide gel, separated by SDS-PAGE, and transferred to a PVDF membrane (Millipore, Billerica, MA, USA). The membranes were blocked in 3% skim milk (FUJIFILM Wako, Osaka, Japan) in Tris-buffered saline-Tween 20 (TBS-T: 20 mM Tris-HCl (pH 7.4), 150 mM NaCl, and 0.1% Tween-20), and incubated with a goat anti-Reelin antibody (AF3820, 1:1,000, R&D Systems, Minneapolis, MN, USA), rat anti-Dab1 (D354-3, 1:1,000, MBL, Nagoya, Japan), or mouse anti-β-actin (sc-47778, 1:1,000, Santa Cruz, Dallas, TX, USA) as a loading control at 4°C overnight. After washing with TBS-T, the membranes were incubated with a peroxidase-labeled anti-goat IgG antibody (HAF109, 1:1,000, R&D Systems), anti-rat IgG (62-9520, 1:10,000, Invitrogen), or anti-mouse IgG (5450-0011, 1:10,000, Sera Care, Milford, MA, USA) at room temperature for 60 min. The immune complex was detected using the ECL Prime Western Blotting Detection reagent (GE Healthcare, Chicago, IL, USA), and protein images were captured by LuminoGraph I (ATTO, Tokyo, Japan).

Regarding WB of Reelin in the conditioned medium, the protein concentration of the conditioned medium was measured by the DC Protein Assay Kit (Bio-Rad Laboratories, Hercules, CA, USA). SDS sample buffer was added to the conditioned medium, and 10 μg of protein samples were loaded onto the 6% SDS polyacrylamide gel. A goat anti-Reelin antibody (AF3820, 1:1,000, R&D Systems) and anti-goat IgG antibody (HAF109, 1:1,000, R&D Systems) were used as the primary and secondary antibodies and to measure the amount of Reelin.

2.8. Immunohistochemistry

Cortical neurons were fixed with 4% paraformaldehyde in 0.1 M phosphate buffer at DIV20 for 20 min, and then incubated in 0.3% Triton X-100 for 10 min. After the incubation in blocking buffer (1% goat serum in PBS) for 30 min, rabbit anti-GABA (A2052-.2ML, 1:1,000, Sigma-Aldrich), rabbit anti-parvalbumin (PV) (ab11427, 1:500, Abcam), mouse anti-Ca^{2+}/calmodulin-dependent protein kinase II α subunit (CaMKIIα) (05-532, 1:1,000, Sigma-Aldrich), goat anti-Reelin (AF3820, 1:1,000, R&D Systems), rabbit anti-MAP2 (AB5622, 1:1,000, Sigma-Aldrich), rabbit anti-GFP (MBL598, 1:500, MBL), and mouse anti-postsynaptic density 95 (PSD95) (MA1-045, 1:500, Invitrogen) antibodies diluted with blocking buffer were added and incubated at 4°C overnight. After washing with PBS, donkey anti-mouse Alexa Fluor (AF) 594 (A21203, 1:1,000, Invitrogen), donkey anti-goat AF 594 (A11058, 1:1,000, Invitrogen), goat anti-rabbit AF 488 (A11034, 1:1,000, Invitrogen), rabbit anti-mouse AF 488 (A21204, 1:1,000, Invitrogen), donkey anti-rabbit AF 488 (A21206, 1:1,000, Invitrogen) antibodies and Hoechst 33342 (346-07951, 1:2,000, Dojindo, Kumamoto, Japan) were added to cortical neurons at

room temperature for 2 h. Confocal images were analyzed using the TiE-A1R Nikon confocal laser microscope (Nikon, Tokyo, Japan). Neuronal marker-positive cells (GABA, PV, and CaMKIIα) were manually counted to identify Reelin-expressing neurons. To analyze the number of PSD95 clusters on MAP2-positive dendrites (25-35 µm from the soma), 3D pictures were constructed from fluorescence images using the Filament Tracer analysis in Imaris (Bitplane, Zurich, Switzerland).

2.9. Live cell imaging

Brightfield images were obtained by IncuCyte ZOOM (Essen Bioscience, Ann Arbor, MI, USA) from DIV3 to DIV7. Neurite lengths and the number of neurite branches were analyzed by the NeuroTrack Analysis Software Module.

2.10. Statistical analysis

Results are expressed as the mean ± standard error of the mean (SEM). Statistical analyses were performed with GraphPad Prism7J (GraphPad Software Inc., San Diego, CA, USA). The significance of differences between two groups was analyzed by the Student's *t*-test. A one-way analysis of variance (ANOVA) and two-way ANOVA, followed by Tukey's multiple comparison test or Dunnett's multiple comparison test were used for more than two groups.

3. Results

3.1. *Reln*-del neurons show reduced Reelin expression levels and intracellular signaling

To investigate the expression levels of Reelin in WT and *Reln*-del cortical neurons at DIV20, we performed WB on intracellular full-length Reelin (FL) and its degradation products (Fig. 1A and 1B). Reelin has eight repeated structures called Reelin repeats (D'Arcangelo et al., 1995). The NR6 fragment is generated by the decomposition of Reelin at the C-t site. NR2 (inactive form) is a fragment that is cleaved at the N-t site of Reelin and does not bind to VLDLR or ApoER2 (Kohno et al., 2009). The expression levels of FL and the NR2 fragment were lower in *Reln*-del$^{+/-}$ neurons than in WT. FL and the NR2 fragment were both barely detectable in *Reln*-del$^{-/-}$ neurons. The expression level of NR6 was significantly decreased in *Reln*-del$^{-/-}$ neurons and slightly reduced in *Reln*-del$^{+/-}$ neurons. The amount of total Reelin, which is the sum of FL, NR6, and NR2 intensities, was also significantly decreased in *Reln*-del$^{+/-}$ and *Reln*-del$^{-/-}$ neurons (FL: $F(2, 12) = 17.71$, $p = 0.0003$, NR6: $F(2, 12) = 5.568$, $p = 0.0195$, NR2: $F(2, 12) = 16.31$, $p = 0.0004$, total Reelin: $F(2, 12) = 16.02$, $p = 0.0004$, Fig. 1C). These results on Reelin expression levels were consistent with previous findings obtained using the whole brains of embryonic and postnatal *Reln*-del mice (Sawahata et al., 2020). We then performed qRT-PCR using primer sets for the conserved and deleted regions in *Reln*-del. Reelin mRNA levels were significantly lower in *Reln*-del$^{+/-}$ mPFC tissue than in WT tissue when either primer set was used for qRT-PCR (Supplementary Fig. 1B and 1C). These results suggest that Reelin protein expression levels were reduced due to the lower expression levels of Reelin mRNA in *Reln*-del neurons.

Since Reelin is secreted extracellularly and binds to receptors for intracellular signal activation (Derer et al., 2001), we also analyzed time-course changes in the amount of secreted Reelin proteins in the conditioned

265 medium of WT and *Reln*-del cortical neurons (Fig. 2A). The trajectories of FL and NR6 levels in the conditioned
266 media of both WT and *Reln*-del$^{+/-}$ neurons increased from DIV3 to DIV10, and then decreased at DIV20, whereas
267 the NR2 fragment accumulated over time (Fig. 2B). Total Reelin, which is the sum of FL, NR6, and NR2 intensities,
268 continued to increase from DIV3 to DIV20 (Fig. 2B). In comparisons of *Reln*-del$^{+/-}$ and WT, *Reln*-del$^{+/-}$ neurons
269 secreted fewer Reelin proteins than WT neurons (Fig. 2B). Furthermore, negligible amounts of Reelin were
270 detected in the conditioned medium of *Reln*-del$^{-/-}$ neurons (Fig. 2C). These results show that Reelin production and
271 secretion were both decreased in *Reln*-del neurons.

272 A previous study reported that phosphorylated Dab1 was rapidly degraded when Reelin signaling was
273 stimulated (Feng et al., 2007). We analyzed changes in intracellular Dab1 expression in primary cultured cortical
274 neurons from WT and *Reln*-del mice at DIV20 (Fig. 3A). Total Dab1 expression levels were significantly higher in
275 *Reln*-del$^{+/-}$ and *Reln*-del$^{-/-}$ neurons than in WT ($F(2, 14) = 17.76$, $p = 0.0001$, Fig. 3B). We confirmed that the
276 expression levels of Dab1 in *Reln*-del$^{+/-}$ neurons were decreased by treatment with 10 nM recombinant Reelin for
277 24 h (vehicle: 1.00 ± 0.06, Reelin: 0.62 ± 0.10, $p < 0.05$, Student's t-test). These findings suggest that intracellular
278 Reelin signaling was diminished in *Reln*-del neurons.

279

280 **3.2. Reelin is mainly produced by GABA-positive neurons in both WT and *Reln*-del$^{+/-}$ mice**

281 We performed immunocytochemistry to identify Reelin-expressing neurons in primary cultured cortical
282 neurons from WT and *Reln*-del$^{+/-}$ mice at DIV20. We found that Reelin was mainly expressed in GABA-positive
283 neurons in both WT ($68.3 \pm 9.0\%$) and *Reln*-del$^{+/-}$ cultures ($66.7 \pm 8.3\%$) (Fig. 4A). No PV-positive neurons

284 expressed Reelin under our experimental conditions (Fig. 4B). CaMKIIα was used as a marker for excitatory
285 neurons (Ma et al., 2019). A small proportion of CaMKIIα-positive excitatory neurons also expressed Reelin (WT
286 neurons: 3.7 ± 3.7%, *Reln*-del$^{+/-}$ neurons: 2.8 ± 2.8%) (Fig. 4C). No significant differences were observed in the
287 types of neurons expressing Reelin between these genotypes.
288
289 **3.3. *Reln*-del neurons show an abnormal neuronal morphology**
290 To examine changes in dendrite elongation and the complexity of *Reln*-del cortical neurons, we analyzed
291 neurite lengths and the number of neurite branches from DIV3 (Fig. 5A) to DIV7 (Fig. 5B) using a live imaging
292 analysis. Neurite lengths and the number of branches were significantly lower in *Reln*-del$^{+/-}$ and *Reln*-del$^{-/-}$ cortical
293 neurons than in WT neurons (time: $F(3, 252) = 161.8$, $p < 0.0001$, genotype: $F(2, 252) = 16.38$, $p < 0.0001$, time ×
294 genotype interaction: $F(6, 252) = 0.3529$, $p = 0.9078$, Fig. 5C; time: $F(3, 252) = 108.3$, $p < 0.0001$, genotype: $F(2,$
295 $252) = 14.59$, $p < 0.0001$, time × genotype interaction: $F(6, 252) = 0.9255$, $p = 0.4771$, Fig. 5D), suggesting some
296 deficits in dendrite development by *Reln*-del neurons.
297 Reelin promotes spine formation, as demonstrated by an increase in the number of PSD95 puncta (Kim et
298 al., 2015), which reflects the postsynaptic density of excitatory synapses (Ibi et al., 2013). We examined the number
299 of dendrites showing PSD95 immunoreactivity using 3D images constructed by serial immunofluorescence images
300 (Fig. 5E). The number of PSD95 puncta was significantly lower in *Reln*-del$^{+/-}$ and *Reln*-del$^{-/-}$ cortical neurons than
301 in WT ($F(2, 33) = 6.859$, $p = 0.0032$, Fig. 5F). These results suggested that deficits in Reelin signaling impaired
302 spine formation and the junction of excitatory synapses in *Reln*-del neurons.

3.4. ADAMTS-3 knockdown may rescue decreased Reelin signaling in *Reln*-del$^{+/-}$ neurons

ADAMTS-3 cleaves Reelin at the N-t site and inactivates extracellular Reelin (Ogino et al., 2017). Therefore, the inhibition of ADAMTS-3 may suppress Reelin degradation and enhance Reelin signaling. To test this assumption, we developed the ADAMTS-3 knockdown method using the lentiviral shRNA vector.

We initially investigated the ADAMTS-3 knockdown efficiency of five candidate shRNA sequences using a primary culture of WT cortical neurons (Supplementary Fig. 2A). High knockdown efficiencies of ADAMTS-3 were obtained with the shRNA#2 and shRNA#3 treatments (90 and 66%, respectively) (Supplementary Fig. 2B). In addition, Reelin cleavage in the conditioned medium of primary cultured cortical neurons with shRNA#2 and shRNA#3 was significantly less than that in the control group (Supplementary Fig. 2C and 2D). The target sequence of shRNA#2 was used in subsequent ADAMTS-3 knockdown experiments.

To label shRNA-expressing neurons with EGFP, we prepared a lentivirus plasmid (shADAMTS-3) using the pLLX vector, in which the target sequence of shRNA#2 was inserted. No significant differences were observed in infection efficiency between the control and ADAMTS-3 knockdown groups (Supplementary Fig. 3A and 3B). ADAMTS-3 mRNA expression levels were markedly decreased at DIV20 in cultured cortical neurons after the transfection with shADAMTS-3 at DIV10. The efficiency of ADAMTS-3 knockdown was estimated to be approximately 84% in cortical neurons (Supplementary Fig. 3C). Like ADAMTS-3, ADAMTS-2 is a protease that inactivates Reelin by cleavage at N-t site (Yamakage et al., 2019). Accordingly, we performed qRT-PCR to check the effect of ADAMTS-3 knockdown on ADAMTS-2 mRNA expression level. There was no significant difference in the

322 expression levels of ADAMTS-2 mRNA between the control group and the ADAMTS-3 knockdown group
323 (Supplementary Fig. 3D).

324 We then investigated the amount of Reelin in the conditioned medium derived from ADAMTS-3
325 knockdown neurons (Fig. 6A). The ratio of FL to total Reelin was significantly increased in the conditioned medium
326 of both WT and *Reln*-del$^{+/-}$ neurons treated with shADAMTS-3 (genotype: $F(1, 16) = 2.033$, $p = 0.1731$, treatment: F
327 $(1, 16) = 27.22$, $p < 0.0001$, genotype × treatment interaction: $F(1, 16) = 0.9929$, $p = 0.3339$, Fig. 6B). Although no
328 significant differences were noted in the ratio of NR6 to total Reelin, the ratio of the NR2 fragment, which is a
329 degradation product of ADAMTS-3, was significantly reduced by the treatment with shADAMTS-3 in both WT
330 and *Reln*-del$^{+/-}$ neurons (Fig. 6C). Further, Dab1 expression levels were significantly lower in WT and *Reln*-del$^{+/-}$
331 neurons treated with shADAMTS-3 than in the respective shControl-treated neurons (genotype: $F(1, 12) = 2.439$, $p =$
332 0.1443, treatment: $F(1, 12) = 38.53$, $p < 0.0001$, genotype × treatment interaction: $F(1, 12) = 0.5299$, $p = 0.4806$, Fig.
333 7A and 7B). These results suggested that the inhibition of ADAMTS-3 using shRNA restored Reelin signaling in
334 *Reln*-del$^{+/-}$ neurons.

335

336 **4. Discussion**

337 We previously reported that *Reln*-del mice that mimic the *RELN* gene defect identified by the
338 genome-wide CNV analysis of schizophrenia patients have abnormalities in their brain structures and social
339 behavior (Sawahata et al., 2020). In the present study, we constructed a primary culture system using the cortical
340 neurons of *Reln*-del mice and analyzed the phenotypes of *Reln*-del neurons. We also examined a method to activate

the Reelin signal by inhibiting the Reelin-degrading enzyme, ADAMTS-3.

We initially demonstrated that the expression of Reelin was reduced in *Reln*-del neurons (Fig. 1 and Fig. 2). Further, the Reelin mRNA levels of mPFC tissue were lower in *Reln*-del$^{+/-}$ mice than in WT mice (Supplementary Fig. 1). On the contrary, a previous study has shown that Orleans *reeler* mutant mice can express a C-terminal truncated Reelin protein, despite having a similar gene deletion to *Reln*-del mice (de Bergeyck et al., 1997). Lower truncated Reelin protein expression levels in *Reln*-del$^{+/-}$ mice may be due to highly unstable Reelin mRNA with *Reln*-del. We measured time-course changes in the amount of secreted Reelin in WT and *Reln*-del$^{+/-}$ cortical neurons (Fig. 2B), and the results obtained on FL and the NR6 fragment in the conditioned medium were similar to previous findings showing that intracellular Reelin expression levels in primary cultured hippocampal neurons increased until DIV12 and decreased after DIV14 (Sinagra et al., 2005). On the other hand, the amount of the NR2 fragment continued to increase in the conditioned medium (Fig. 2B). The NR2 fragment is generated from FL and the NR6 fragment by the N-t site degradation of secreted metalloproteinases, such as ADAMTS-3 (Ogino et al., 2017), and also potentially by endosome degradation and re-secretion following the endocytosis of Reelin (Hibi and Hattori, 2009). Therefore, the NR2 fragment appeared to accumulate in the conditioned medium even though FL and NR6 fragment expression levels were decreased, resulting in an increase in total Reelin levels.

After phosphorylation by the Reelin stimulation, Dab1 is polyubiquitinated and degraded via the proteasome pathway (Arnaud et al., 2003). The Dab1 protein in Reelin-deficient mice accumulates intracellularly because Dab1 is not degraded without Reelin signaling (Martin-Lopez et al., 2011). Although phosphorylated level of Dab1 should be monitored in the present study, there was no prominent anti-phosphorylated Dab1 antibody.

Therefore, we analyzed Dab1 expression level instead of phosphorylated Dab1 to monitor the activity of the Reelin signal. Dab1 expression levels were significantly higher in *Reln*-del neurons than in WT neurons (Fig. 3B). These results indicated that Reelin signaling was decreased in *Reln*-del neurons. Further studies are needed to investigate signal activity downstream of Dab1, such as the phosphatidylinositol 3-kinase (PI3K)/Akt pathway (Jossin and Goffinet, 2007).

Regarding WT and *Reln*-del$^{+/-}$ primary cultured cortical neurons, more than 60% of GABA-positive inhibitory neurons expressed Reelin (Fig. 4A), whereas Reelin was not detected in PV-positive interneurons (Fig. 4B). These results on Reelin expression in GABA- and PV-positive neurons are consistent with previous findings in the adult rat brain (Pesold et al., 1998; Pesold et al., 1999). A previous study reported that Reelin was expressed in inhibitory neurons with neuropeptide Y and somatostatin (Pesold et al., 1999). Reelin was also suggested to be weakly expressed in excitatory neurons (Carceller et al., 2016); however, limited information is currently available on Reelin production in non-GABAergic neurons. We also found that a few CaMKIIα-positive cells expressed the Reelin protein in primary cultured cortical neurons from both WT and *Reln*-del$^{+/-}$ mice, suggesting that Reelin is also expressed by a small proportion of excitatory neurons (Fig. 4C). No changes were observed in the proportion of Reelin-expressing cells in GABA-, PV-, or CaMKIIα-positive cells between WT and *Reln*-del$^{+/-}$ cortical neurons. Further studies are needed to characterize Reelin-expressing CaMKIIα-positive cortical neurons in culture.

Reelin controls dendrite development in the brain. *Reeler* mice, a type of Reelin-deficient mouse, have shorter hippocampal dendrites (Niu et al., 2004). Reelin activates intracellular signaling, which affects dendrite development and neuronal migration, such as PI3K and Akt, through Dab1 phosphorylation (Beffert et al., 2002).

379 Live cell imaging showed that primary cultured *Reln*-del cortical neurons had a shorter neurite length (Fig. 5C) and
380 fewer neurite branches than WT neurons (Fig. 5D).

381 Previous studies indicated that Reelin also facilitated spine formation (Niu et al., 2008) and regulated the
382 number of PSD95 puncta to increase spine density (Kim et al., 2015). Reelin is secreted by GABA-positive neurons
383 and acts by binding to Reelin receptors present on the cell membrane of nearby neurons. Reelin also promotes spine
384 formation by an increase in the number of PSD95 puncta (Kim et al., 2015). The activation of ApoER2 and
385 VLDLR present in excitatory synapses by Reelin increases Dab1 phosphorylation and activates Src, and
386 subsequently promotes Src binding to PSD-95. Then, phosphorylation of the NMDA receptor subunit physically
387 associated with PSD95 is increased, resulting in activation of the NMDA receptor (Beffert et al., 2005; Qiu et al.,
388 2006). Based on clinical observations showing that spine density was lower in schizophrenia patients than in
389 control subjects (Glantz and Lewis, 2000), we performed an immunocytochemical analysis of spine formation in
390 WT and *Reln*-del cortical neurons to examine the number of PSD95 puncta on MAP2-positive dendrites (Ibi et al.,
391 2013). The results obtained revealed that the number of PSD95 puncta was significantly lower in *Reln*-del neurons
392 than in WT neurons (Fig. 5F) when these neurons were cultured in Neurobasal medium containing B-27
393 supplement and GlutaMax-I. We also confirmed that there were no significant differences in the ratio of
394 CaMKIIα-positive excitatory neurons (WT: 41.6 ± 5.0%, *Reln*-del$^{+/-}$: 36.8 ± 5.8% of total cells, p = 0.5383,
395 Student's *t*-test) and GABA-positive inhibitory neurons (WT: 44.6 ± 6.1%, *Reln*-del$^{+/-}$: 38.6 ± 6.0% of total cells, p
396 = 0.4959, Student's *t*-test) between WT and *Reln*-del$^{+/-}$ neurons in the same experimental conditions. These results
397 suggested that impairments in neurite and spine formation during neurodevelopment contribute in part to brain

398 structural abnormalities in *Reln*-del mice.

399 ADAMTS are a family of secreted proteases that are involved in collagen processing and matrix
400 proteoglycan cleavage (Porter et al., 2005). Within the ADAMTS group, ADAMTS-3 exhibits stronger cleavage
401 activity at the N-t site of Reelin *in vivo* (Yamakage et al., 2019). We performed ADAMTS-3 knockdown
402 experiments using shRNA in WT and *Reln*-del$^{+/-}$ neurons and succeeded in efficiently introducing shRNA into
403 primary cultured cortical neurons and knocking down ADAMTS-3 using a lentivirus system (Supplementary Fig. 3).
404 The knockdown of ADMATS-3 in WT neurons suppressed Reelin degradation (Fig. 6B) and decreased intracellular
405 Dab1 levels (Fig. 7B), suggesting that Reelin signaling in WT neurons was enhanced by the inhibition of
406 ADAMTS-3. A previous study using ADAMTS-3 cKO mice with an ADAMTS-3 deficiency only in the excitatory
407 neurons of the forebrain showed reductions in Reelin cleavage and Dab1 expression levels in the cerebral cortex and
408 hippocampus (Ogino et al., 2017). The results obtained in the lentivirus-mediated ADAMTS-3 knockdown
409 experiment on primary cultured neurons are consistent with the changes observed in the brains of ADMATS-3 cKO
410 mice. We also showed that the inhibition of ADAMTS-3 effectively improved Reelin signaling in *Reln*-del$^{+/-}$ neurons
411 with low Reelin expression levels (Fig. 6 and Fig. 7). Since we analyzed only Dab1 level as Reelin signaling
412 molecules in this study, further experiments are required to investigate whether ADAMTS-3 knockdown can improve
413 the alterations of downstream signaling, and ameliorate the impairments in neurite and spine formation in *Reln*-del$^{+/-}$
414 neurons.

415 Decreased Reelin levels have been shown to induce behavioral impairments in pre-pulse inhibition,
416 contextual fear conditioned learning, anxiety, social behavior, and motor learning (Qiu et al., 2006; Sobue et al.,

2018). Furthermore, Reelin supplementation enhanced associative learning and increased pre-pulse inhibition in *Reeler* mice (Rogers et al., 2013). Reelin injections into the hippocampus of polyI:C-treated MIA model mice improved their cognitive deficits and anxiety-like behavior (Ibi et al., 2020). The present results taken together with these previous findings on Reelin supplementation show that the ADAMTS-3 knockdown method is a potential candidate for the clinical treatment of neuropsychological disorders, such as schizophrenia, by suppressing the degradation of endogenous Reelin. To develop new treatments for schizophrenia based on Reelin signaling enhancements, we need to investigate whether the knockdown of ADAMTS-3 improves behavioral and morphological abnormalities in *Reln*-del mice.

One might concern that Reelin replacement therapy may be effective for the treatment only in a very minor population of schizophrenia patients with *RELN* deletion, but not in most of the patients without *RELN* deletion. In this regard, it has already been reported that the expression of Reelin mRNA in the brain and peripheral blood of schizophrenia patients tends to decrease compared to healthy control (Yin et al., 2020). Similarly, Reelin expression level is reduced in the hippocampus of MIA mouse model of schizophrenia, which is not directly related to the *RELN* mutation, and their cognitive impairment as well as anxiety-like behavior are ameliorated by the intrahippocampal administration of Reelin (Ibi et al., 2020). Reelin overexpression prevents pre-pulse inhibition deficits induced by MK-801, a NMDA receptor antagonist (Teixeira et al., 2011). Alternatively, it is reported that Reelin supplementation can improve the cognitive function in WT mice (Rogers et al., 2011). Accordingly, it is conceivable that Reelin replacement therapy including ADAMTS-3 inhibition may be effective not only for schizophrenia patients with *RELN* deletion, but also for the patients without *RELN* deletion.

436

437

438 **5. Conclusion**

439 In primary cultured cortical neurons from *Reln*-del mice, the protein levels of intracellular and
440 extracellular Reelin were lower, while Dab1 levels were higher than those in WT mice. These results suggest that
441 Reelin signaling is weaker in *Reln*-del neurons than in WT neurons. *Reln*-del neurons had shorter neurites and
442 fewer branch points than WT neurons. Furthermore, the number of PSD95 clusters on MAP2-positive dendrites
443 was decreased in *Reln*-del neurons. The inhibition of ADAMTS-3 may augment Reelin signaling by suppressing
444 secreted Reelin cleavage not only in WT neurons, but also in *Reln*-del neurons. We propose a novel concept to
445 enhance Reelin signaling, namely, the inhibition of ADAMTS-3, as a new treatment for patients with
446 schizophrenia.

447

448 **Acknowledgments**

449 This work was supported by AMED under Grants JP20dm0107087, JSPS KAKENHI Grant Number JP17H04252
450 and JP20H03428 and The Uehara Memorial Foundation.

451

452 **Figure legends**

453 **Fig. 1. Comparison of intracellular Reelin expression levels in WT and *Reln*-del neurons.** (A) Schematic
454 representation of full-length Reelin (FL), NR6 (the C-t site cleaved fragment), and NR2 (the N-t site cleaved

455 fragment). (B) Western blotting (WB) of intracellular FL and the NR6 and NR2 fragments of primary cortical
456 neurons from WT, *Reln*-del$^{+/-}$ (+/-), and *Reln*-del$^{-/-}$ (-/-) mice at 20 days *in vitro* (DIV20). (C) Quantification of
457 intracellular FL, NR6, NR2, and total Reelin (Sum of FL, NR6, and NR2 intensities). Data represent the mean ±
458 SEM (n = 5 for WT; n = 6 for *Reln*-del$^{+/-}$; n = 4 for *Reln*-del$^{-/-}$) and were analyzed by Tukey's multiple comparison
459 test. *p < 0.05 and ***p < 0.001.

460

461 **Fig. 2. Comparison of Reelin protein levels in the conditioned medium of WT and *Reln*-del neurons.** (A) WB
462 analysis of FL and the NR6 and NR2 fragments in the conditioned medium of primary cortical neurons from WT
463 and *Reln*-del$^{+/-}$ mice from DIV3 to DIV20, and from *Reln*-del$^{-/-}$ mice at DIV20. (B) The amounts of FL, NR6, NR2,
464 and total Reelin in the conditioned medium of WT and *Reln*-del$^{+/-}$ mice cortical neurons from DIV3 to DIV20. Data
465 represent the mean ± SEM (n = 4) and were analyzed by the Student's *t*-test at each time point. *p < 0.05 and **p <
466 0.01. (C) Quantification of FL, NR6, NR2, and total Reelin in the conditioned medium of WT and *Reln*-del$^{-/-}$ mouse
467 cortical neurons at DIV20. Data represent the mean ± SEM (n = 3) and were analyzed by the Student's *t*-test at each
468 time point. *p < 0.05, ***p < 0.001, and ****p < 0.0001.

469

470 **Fig. 3. Analysis of Dab1 expression levels in WT and *Reln*-del neurons.** (A) WB of Dab1 in primary cortical
471 neurons from WT, *Reln*-del$^{+/-}$, and *Reln*-del$^{-/-}$ mice at DIV20. (B) Quantification of intracellular Dab1. Data
472 represent the mean ± SEM (n = 6 for WT; n = 7 for *Reln*-del$^{+/-}$; n = 4 for *Reln*-del$^{-/-}$) and were analyzed by Tukey's
473 multiple comparison test. *p < 0.05, **p < 0.01, and ****p < 0.0001.

Fig. 4. Immunofluorescence images showing Reelin expression in cortical neurons from WT and *Reln*-del$^{+/-}$ mice. (A) Representative immunofluorescence images labeled for GABA (green) and Reelin (red). (B) Representative immunofluorescence images labeled for parvalbumin (PV, green) and Reelin (red). (C) Representative immunofluorescence images labeled for CaMKIIα (green) and Reelin (red). Nuclei were stained with Hoechst 33342 (blue). Nine pictures (3 pictures from one mouse) were obtained in each group (n = 3). Scale bar: 100 µm.

Fig. 5. Morphological analysis of primary cultured cortical neurons from WT and *Reln*-del mice. (A, B) Representative time-lapse images of cortical neurons from WT, *Reln*-del$^{+/-}$, and *Reln*-del$^{-/-}$ mice at DIV 3 (A) and DIV7 (B). (C, D) Graph of analyses of neurite lengths (C) and neurite branch points (D). Data represent the mean ± SEM (n = 12-16 for WT; n = 20-22 for *Reln*-del$^{+/-}$; n = 6 for *Reln*-del$^{-/-}$) and were analyzed by a two-way ANOVA. *$p < 0.05$ and **$p < 0.01$, *Reln*-del$^{+/-}$ and *Reln*-del$^{-/-}$ versus WT. (E, left) Representative images of immunocytochemistry for MAP2-positive dendrites (green), PSD95 puncta (red), and nuclei stained with Hoechst 33342 (blue). (E, right) 3D images constructed from immunofluorescence data at DIV20. (F) Number of PSD95 clusters on MAP2-positive dendrites in WT, *Reln*-del$^{+/-}$, and *Reln*-del$^{-/-}$ neurons. Data represent the mean ± SEM (n = 4 for WT; n = 5 for *Reln*-del$^{+/-}$; n = 4 for *Reln*-del$^{-/-}$). Twenty neurons were obtained from each group and analyzed by Tukey's multiple comparison test. *$p < 0.05$, **$p < 0.01$. Scale bar: 25 µm.

Fig. 6. Effects of ADAMTS-3 knockdown on Reelin cleavage in the conditioned medium of WT and *Reln*-del$^{+/-}$ neurons. (A) WB of full-length Reelin (FL) and the NR6 and NR2 fragments in the conditioned medium of primary cortical neurons from WT and *Reln*-del$^{+/-}$ mice. Neurons were treated with a lentivirus containing control shRNA (shControl) or shRNA targets ADAMTS-3 (shADAMTS-3) at DIV10, and the conditioned medium was then analyzed at DIV20. (B) Ratio of FL, NR6, and NR2 to total Reelin (Sum of FL, NR6 and NR2 intensities). Data represent the mean ± SEM (n = 5 in each group) and were analyzed by a two-way ANOVA. *p < 0.05, **p < 0.01. (C) The summary for the ratio of the Reelin fragment fraction.

Fig. 7. Effects of the ADAMTS-3 knockdown on Dab1 expression levels in WT and *Reln*-del$^{+/-}$ neurons. (A) WB of Dab1 in primary cortical neurons from WT and *Reln*-del$^{+/-}$ mice. Neurons were treated with a lentivirus containing control shRNA or shADAMTS-3 at DIV10, and were then analyzed at DIV20. (B) Quantification of intracellular Dab1. Data represent the mean ± SEM (n = 4 in each group) and were analyzed by a two-way ANOVA. *p < 0.05, **p < 0.01.

References

Arnaud, L., Ballif, B.A., Cooper, J.A., 2003. Regulation of protein tyrosine kinase signaling by substrate degradation during brain development. Mol Cell Biol 23, 9293-9302.

Beffert, U., Morfini, G., Bock, H.H., Reyna, H., Brady, S.T., Herz, J., 2002. Reelin-mediated signaling locally regulates protein kinase B/Akt and glycogen synthase kinase 3beta. J Biol Chem 277, 49958-49964.

512 Beffert, U., Weeber, E.J., Durudas, A., Qiu, S., Masiulis, I., Sweatt, J.D., Li, W.P., Adelmann, G., Frotscher, M.,
513 Hammer, R.E., Herz, J., 2005. Modulation of synaptic plasticity and memory by Reelin involves differential
514 splicing of the lipoprotein receptor Apoer2. Neuron 47, 567-579.
515 Benhayon, D., Magdaleno, S., Curran, T., 2003. Binding of purified Reelin to ApoER2 and VLDLR mediates
516 tyrosine phosphorylation of Disabled-1. Brain Res Mol Brain Res 112, 33-45.
517 Bock, H.H., Herz, J., 2003. Reelin activates SRC family tyrosine kinases in neurons. Curr Biol 13, 18-26.
518 Carceller, H., Rovira-Esteban, L., Nacher, J., Castren, E., Guirado, R., 2016. Neurochemical phenotype of Reelin
519 immunoreactive cells in the piriform cortex layer II. Front Cell Neurosci 10, 65.
520 Chen, Y., Beffert, U., Ertunc, M., Tang, T.S., Kavalali, E.T., Bezprozvanny, I., Herz, J., 2005. Reelin modulates
521 NMDA receptor activity in cortical neurons. J Neurosci 25, 8209-8216.
522 Curran, T., D'Arcangelo, G., 1998. Role of reelin in the control of brain development. Brain Res Brain Res Rev 26,
523 285-294.
524 D'Arcangelo, G., Miao, G.G., Chen, S.C., Soares, H.D., Morgan, J.I., Curran, T., 1995. A protein related to
525 extracellular matrix proteins deleted in the mouse mutant reeler. Nature 374, 719-723.
526 de Bergeyck, V., Nakajima, K., Lambert de Rouvroit, C., Naerhuyzen, B., Goffinet, A.M., Miyata, T., Ogawa, M.,
527 Mikoshiba, K., 1997. A truncated Reelin protein is produced but not secreted in the 'Orleans' reeler mutation
528 (Reln[rl-Orl]). Brain Res Mol Brain Res 50, 85-90.
529 Derer, P., Derer, M., Goffinet, A., 2001. Axonal secretion of Reelin by Cajal-Retzius cells: evidence from
530 comparison of normal and Reln(Orl) mutant mice. J Comp Neurol 440, 136-143.

Feng, L., Allen, N.S., Simo, S., Cooper, J.A., 2007. Cullin 5 regulates Dab1 protein levels and neuron positioning during cortical development. Genes Dev 21, 2717-2730.

Glantz, L.A., Lewis, D.A., 2000. Decreased dendritic spine density on prefrontal cortical pyramidal neurons in schizophrenia. Arch Gen Psychiatry 57, 65-73.

Hartfuss, E., Forster, E., Bock, H.H., Hack, M.A., Leprince, P., Luque, J.M., Herz, J., Frotscher, M., Gotz, M., 2003. Reelin signaling directly affects radial glia morphology and biochemical maturation. Development 130, 4597-4609.

Hibi, T., Hattori, M., 2009. The N-terminal fragment of Reelin is generated after endocytosis and released through the pathway regulated by Rab11. FEBS Lett 583, 1299-1303.

Ibi, D., Nagai, T., Nakajima, A., Mizoguchi, H., Kawase, T., Tsuboi, D., Kano, S., Sato, Y., Hayakawa, M., Lange, U.C., Adams, D.J., Surani, M.A., Satoh, T., Sawa, A., Kaibuchi, K., Nabeshima, T., Yamada, K., 2013. Astroglial IFITM3 mediates neuronal impairments following neonatal immune challenge in mice. Glia 61, 679-693.

Ibi, D., Nakasai, G., Koide, N., Sawahata, M., Kohno, T., Takaba, R., Nagai, T., Hattori, M., Nabeshima, T., Yamada, K., Hiramatsu, M., 2020. Reelin supplementation into the hippocampus rescues abnormal behavior in a mouse model of neurodevelopmental disorders. Front Cell Neurosci 14, 285.

Impagnatiello, F., Guidotti, A.R., Pesold, C., Dwivedi, Y., Caruncho, H., Pisu, M.G., Uzunov, D.P., Smalheiser, N.R., Davis, J.M., Pandey, G.N., Pappas, G.D., Tueting, P., Sharma, R.P., Costa, E., 1998. A decrease of reelin expression as a putative vulnerability factor in schizophrenia. Proc Natl Acad Sci U S A 95, 15718-15723.

550 Jossin, Y., Goffinet, A.M., 2007. Reelin signals through phosphatidylinositol 3-kinase and Akt to control cortical
551 development and through mTor to regulate dendritic growth. Mol Cell Biol 27, 7113-7124.
552 Kim, M., Jeong, Y., Chang, Y.C., 2015. Extracellular matrix protein reelin regulate dendritic spine density through
553 CaMKIIbeta. Neurosci Lett 599, 97-101.
554 Kohno, S., Kohno, T., Nakano, Y., Suzuki, K., Ishii, M., Tagami, H., Baba, A., Hattori, M., 2009. Mechanism and
555 significance of specific proteolytic cleavage of Reelin. Biochem Biophys Res Commun 380, 93-97.
556 Koie, M., Okumura, K., Hisanaga, A., Kamei, T., Sasaki, K., Deng, M., Baba, A., Kohno, T., Hattori, M., 2014.
557 Cleavage within Reelin repeat 3 regulates the duration and range of the signaling activity of Reelin protein. J
558 Biol Chem 289, 12922-12930.
559 Kushima, I., Aleksic, B., Nakatochi, M., Shimamura, T., Shiino, T., Yoshimi, A., Kimura, H., Takasaki, Y., Wang,
560 C., Xing, J., Ishizuka, K., Oya-Ito, T., Nakamura, Y., Arioka, Y., Maeda, T., Yamamoto, M., Yoshida, M.,
561 Noma, H., Hamada, S., Morikawa, M., Uno, Y., Okada, T., Iidaka, T., Iritani, S., Yamamoto, T., Miyashita, M.,
562 Kobori, A., Arai, M., Itokawa, M., Cheng, M.C., Chuang, Y.A., Chen, C.H., Suzuki, M., Takahashi, T.,
563 Hashimoto, R., Yamamori, H., Yasuda, Y., Watanabe, Y., Nunokawa, A., Someya, T., Ikeda, M., Toyota, T.,
564 Yoshikawa, T., Numata, S., Ohmori, T., Kunimoto, S., Mori, D., Iwata, N., Ozaki, N., 2017. High-resolution
565 copy number variation analysis of schizophrenia in Japan. Mol Psychiatry 22, 430-440.
566 Lois, C., Hong, E.J., Pease, S., Brown, E.J., Baltimore, D., 2002. Germline transmission and tissue-specific
567 expression of transgenes delivered by lentiviral vectors. Science 295, 868-872.
568 Ma, J., Zhang, L.Q., He, Z.X., He, X.X., Wang, Y.J., Jian, Y.L., Wang, X., Zhang, B.B., Su, C., Lu, J., Huang, B.Q.,

Zhang, Y., Wang, G.Y., Guo, W.X., Qiu, D.L., Mei, L., Xiong, W.C., Zheng, Y.W., Zhu, X.J., 2019. Autism candidate gene DIP2A regulates spine morphogenesis via acetylation of cortactin. PLoS Biol 17, e3000461.

Martin-Lopez, E., Blanchart, A., De Carlos, J.A., Lopez-Mascaraque, L., 2011. Dab1 (Disable homolog-1) reelin adaptor protein is overexpressed in the olfactory bulb at early postnatal stages. PLoS One 6, e26673.

Meyer, G., Goffinet, A.M., Fairen, A., 1999. What is a Cajal-Retzius cell? A reassessment of a classical cell type based on recent observations in the developing neocortex. Cereb Cortex 9, 765-775.

Niu, S., Renfro, A., Quattrocchi, C.C., Sheldon, M., D'Arcangelo, G., 2004. Reelin promotes hippocampal dendrite development through the VLDLR/ApoER2-Dab1 pathway. Neuron 41, 71-84.

Niu, S., Yabut, O., D'Arcangelo, G., 2008. The Reelin signaling pathway promotes dendritic spine development in hippocampal neurons. J Neurosci 28, 10339-10348.

Ogino, H., Hisanaga, A., Kohno, T., Kondo, Y., Okumura, K., Kamei, T., Sato, T., Asahara, H., Tsuiji, H., Fukata, M., Hattori, M., 2017. Secreted metalloproteinase ADAMTS-3 inactivates Reelin. J Neurosci 37, 3181-3191.

Pesold, C., Impagnatiello, F., Pisu, M.G., Uzunov, D.P., Costa, E., Guidotti, A., Caruncho, H.J., 1998. Reelin is preferentially expressed in neurons synthesizing gamma-aminobutyric acid in cortex and hippocampus of adult rats. Proc Natl Acad Sci U S A 95, 3221-3226.

Pesold, C., Liu, W.S., Guidotti, A., Costa, E., Caruncho, H.J., 1999. Cortical bitufted, horizontal, and Martinotti cells preferentially express and secrete reelin into perineuronal nets, nonsynaptically modulating gene expression. Proc Natl Acad Sci U S A 96, 3217-3222.

Porter, S., Clark, I.M., Kevorkian, L., Edwards, D.R., 2005. The ADAMTS metalloproteinases. Biochem J 386,

15-27.

Qiu, S., Korwek, K.M., Pratt-Davis, A.R., Peters, M., Bergman, M.Y., Weeber, E.J., 2006. Cognitive disruption and altered hippocampus synaptic function in Reelin haploinsufficient mice. Neurobiol Learn Mem 85, 228-242.

Qiu, S., Zhao, L.F., Korwek, K.M., Weeber, E.J., 2006. Differential reelin-induced enhancement of NMDA and AMPA receptor activity in the adult hippocampus. J Neurosci 26, 12943-12955.

Rogers, J.T., Rusiana, I., Trotter, J., Zhao, L., Donaldson, E., Pak, D.T., Babus, L.W., Peters, M., Banko, J.L., Chavis, P., Rebeck, G.W., Hoe, H.S., Weeber, E.J., 2011. Reelin supplementation enhances cognitive ability, synaptic plasticity, and dendritic spine density. Learn Mem 18, 558-564.

Rogers, J.T., Zhao, L., Trotter, J.H., Rusiana, I., Peters, M.M., Li, Q., Donaldson, E., Banko, J.L., Keenoy, K.E., Rebeck, G.W., Hoe, H.S., D'Arcangelo, G., Weeber, E.J., 2013. Reelin supplementation recovers sensorimotor gating, synaptic plasticity and associative learning deficits in the heterozygous reeler mouse. J Psychopharmacol 27, 386-395.

Sawahata, M., Mori, D., Arioka, Y., Kubo, H., Kushima, I., Kitagawa, K., Sobue, A., Shishido, E., Sekiguchi, M., Kodama, A., Ikeda, R., Aleksic, B., Kimura, H., Ishizuka, K., Nagai, T., Kaibuchi, K., Nabeshima, T., Yamada, K., Ozaki, N., 2020. Generation and analysis of novel Reln-deleted mouse model corresponding to exonic Reln deletion in schizophrenia. Psychiatry Clin Neurosci 74, 318-327.

Schramek, D., Sendoel, A., Segal, J.P., Beronja, S., Heller, E., Oristian, D., Reva, B., Fuchs, E., 2014. Direct in vivo RNAi screen unveils myosin IIa as a tumor suppressor of squamous cell carcinomas. Science 343, 309-313.

607 Sinagra, M., Verrier, D., Frankova, D., Korwek, K.M., Blahos, J., Weeber, E.J., Manzoni, O.J., Chavis, P., 2005.
608 Reelin, very-low-density lipoprotein receptor, and apolipoprotein E receptor 2 control somatic NMDA
609 receptor composition during hippocampal maturation in vitro. J Neurosci 25, 6127-6136.
610 Sobue, A., Kushima, I., Nagai, T., Shan, W., Kohno, T., Aleksic, B., Aoyama, Y., Mori, D., Arioka, Y., Kawano, N.,
611 Yamamoto, M., Hattori, M., Nabeshima, T., Yamada, K., Ozaki, N., 2018. Genetic and animal model analyses
612 reveal the pathogenic role of a novel deletion of RELN in schizophrenia. Sci Rep 8, 13046.
613 Teixeira, C.M., Martin, E.D., Sahun, I., Masachs, N., Pujadas, L., Corvelo, A., Bosch, C., Rossi, D., Martinez, A.,
614 Maldonado, R., Dierssen, M., Soriano, E., 2011. Overexpression of Reelin prevents the manifestation of
615 behavioral phenotypes related to schizophrenia and bipolar disorder. Neuropsychopharmacology 36,
616 2395-2405.
617 Tissir, F., Goffinet, A.M., 2003. Reelin and brain development. Nat Rev Neurosci 4, 496-505.
618 Tsujimura, K., Irie, K., Nakashima, H., Egashira, Y., Fukao, Y., Fujiwara, M., Itoh, M., Uesaka, M., Imamura, T.,
619 Nakahata, Y., Yamashita, Y., Abe, T., Takamori, S., Nakashima, K., 2015. miR-199a Links MeCP2 with mTOR
620 signaling and its dysregulation leads to Rett syndrome phenotypes. Cell Rep 12, 1887-1901.
621 Wasser, C.R., Herz, J., 2017. Reelin: Neurodevelopmental architect and homeostatic regulator of excitatory
622 synapses. J Biol Chem 292, 1330-1338.
623 Weeber, E.J., Beffert, U., Jones, C., Christian, J.M., Forster, E., Sweatt, J.D., Herz, J., 2002. Reelin and ApoE
624 receptors cooperate to enhance hippocampal synaptic plasticity and learning. J Biol Chem 277, 39944-39952.
625 Yamakage, Y., Kato, M., Hongo, A., Ogino, H., Ishii, K., Ishizuka, T., Kamei, T., Tsuiji, H., Miyamoto, T., Oishi, H.,

626 Kohno, T., Hattori, M., 2019. A disintegrin and metalloproteinase with thrombospondin motifs 2 cleaves and
627 inactivates Reelin in the postnatal cerebral cortex and hippocampus, but not in the cerebellum. Mol Cell
628 Neurosci 100, 103401.
629 Yin, J., Lu, Y., Yu, S., Dai, Z., Zhang, F., Yuan, J., 2020. Exploring the mRNA expression level of RELN in
630 peripheral blood of schizophrenia patients before and after antipsychotic treatment. Hereditas 157.
631 Zhou, Z., Hong, E.J., Cohen, S., Zhao, W.N., Ho, H.Y., Schmidt, L., Chen, W.G., Lin, Y., Savner, E., Griffith, E.C.,
632 Hu, L., Steen, J.A., Weitz, C.J., Greenberg, M.E., 2006. Brain-specific phosphorylation of MeCP2 regulates
633 activity-dependent Bdnf transcription, dendritic growth, and spine maturation. Neuron 52, 255-269.

Figure 1

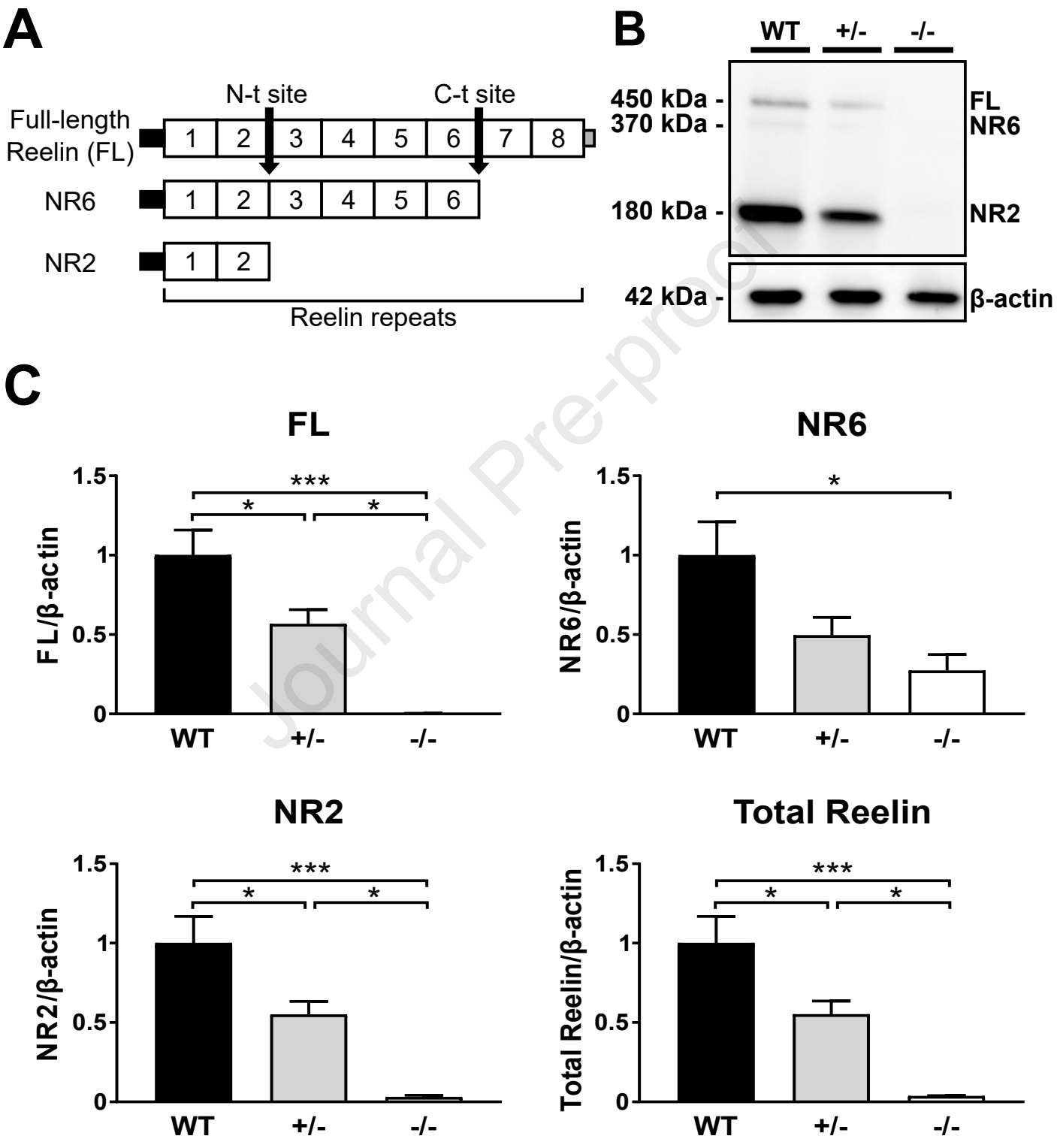

Figure 2 (A-B)

A

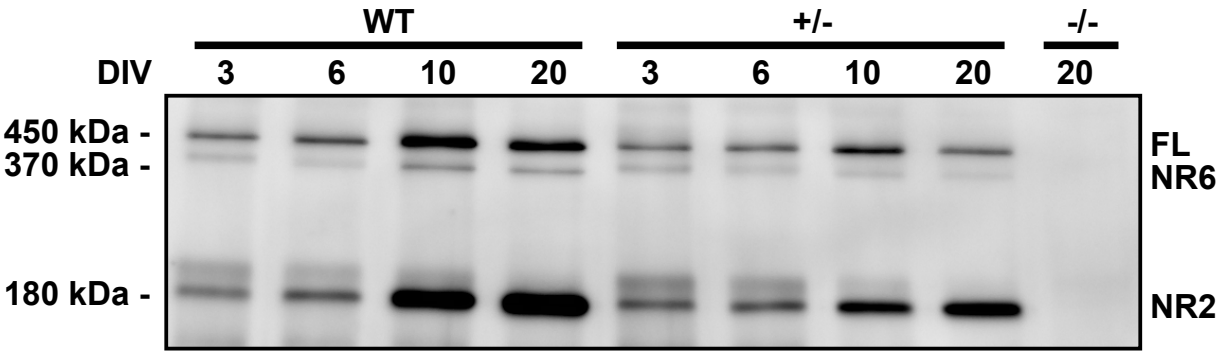

B

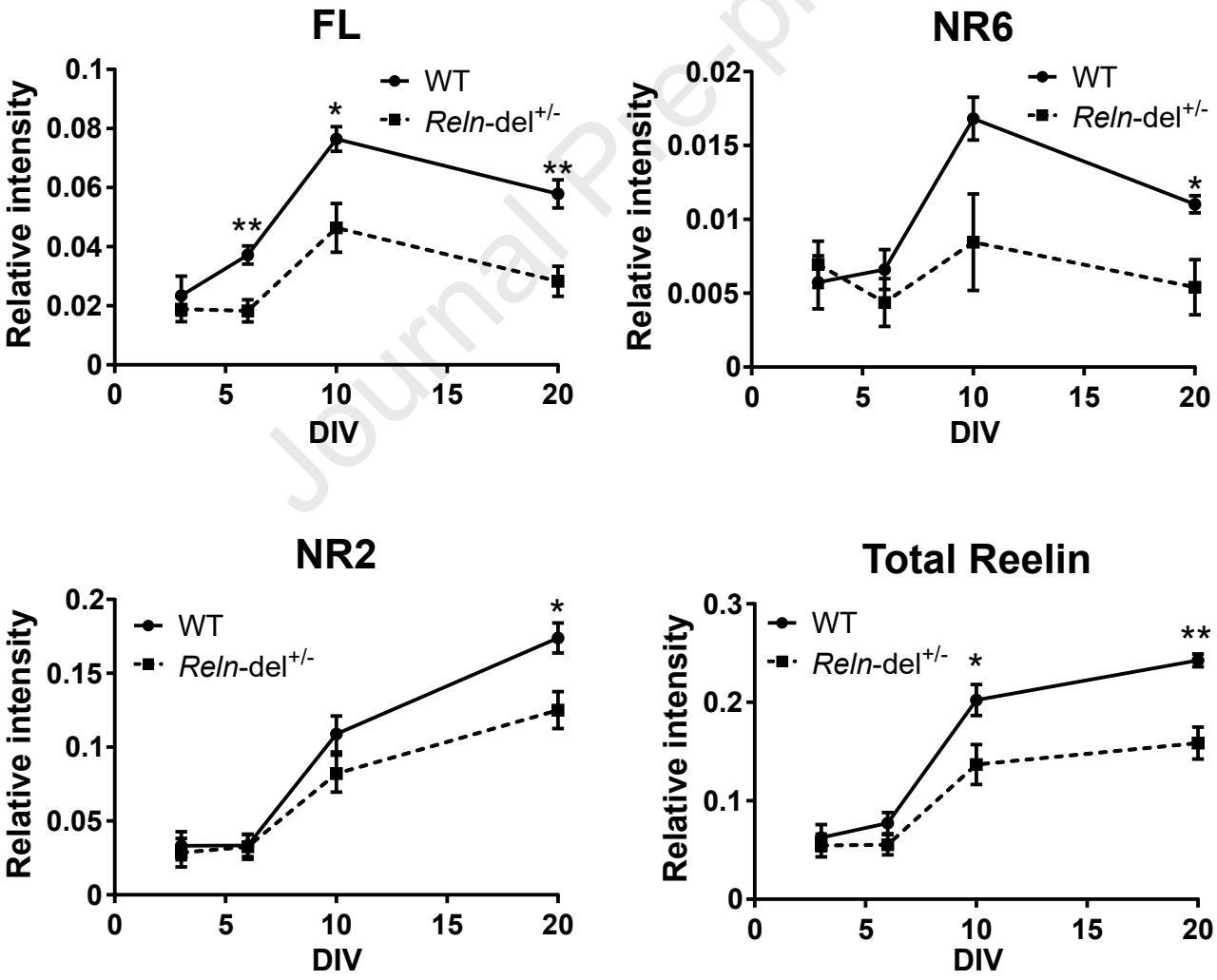

Figure 2 (C)

C

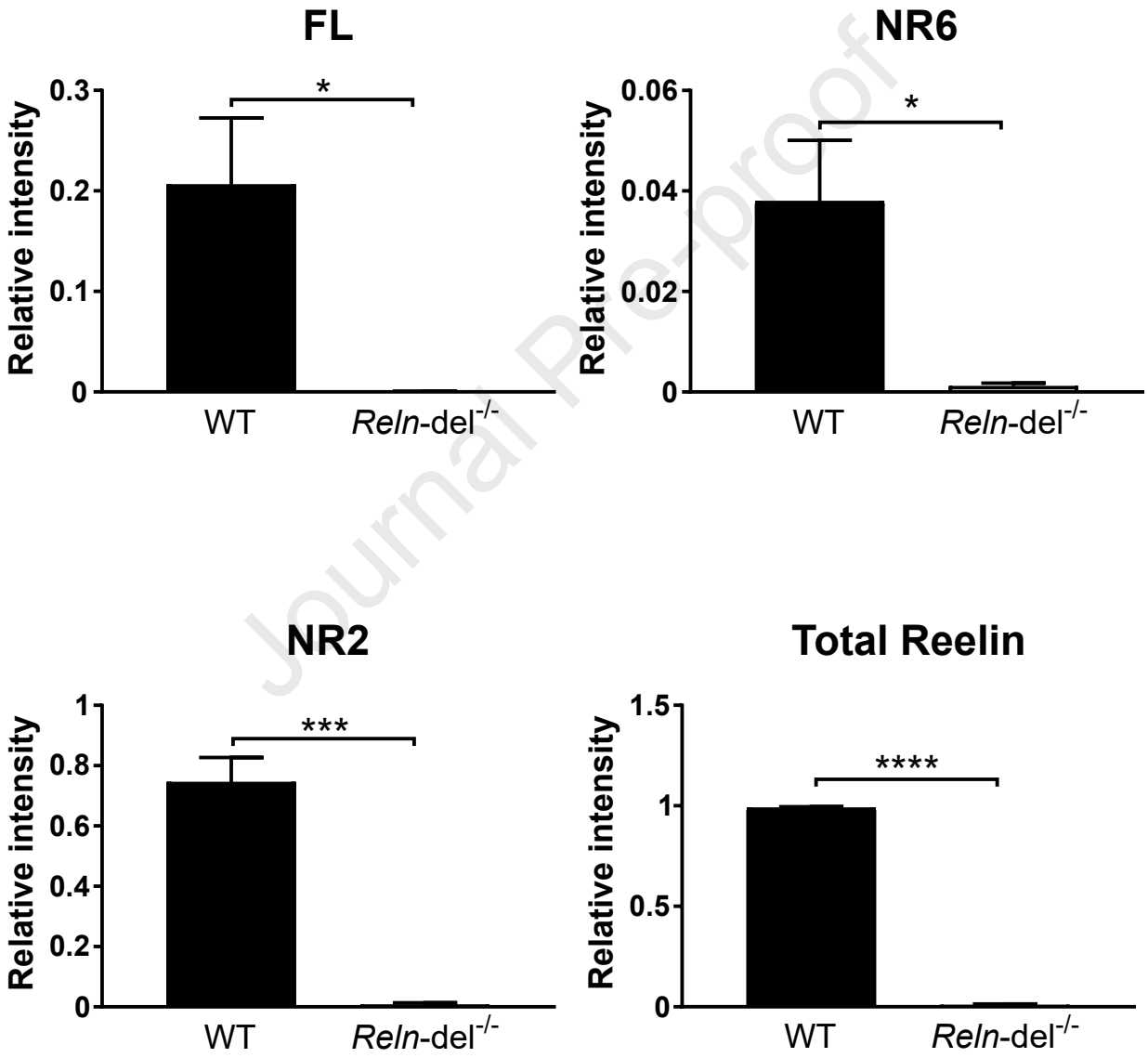

Figure 3

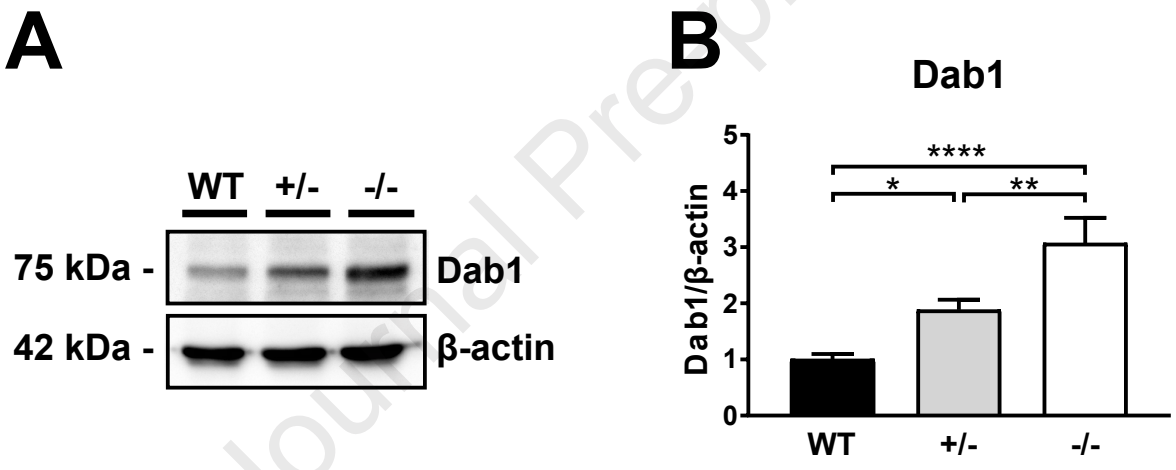

Figure 4

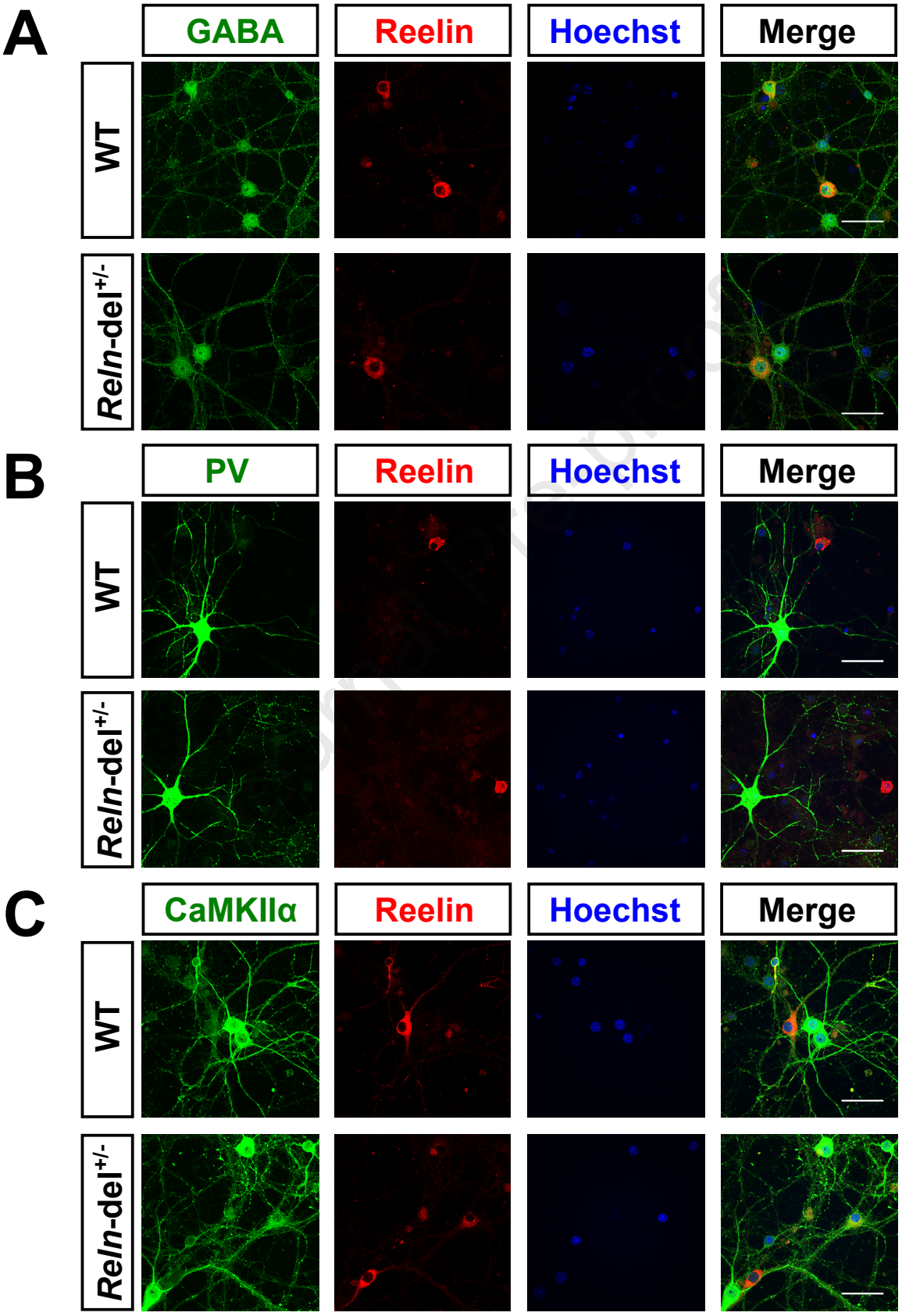

Figure 5 (A-D)

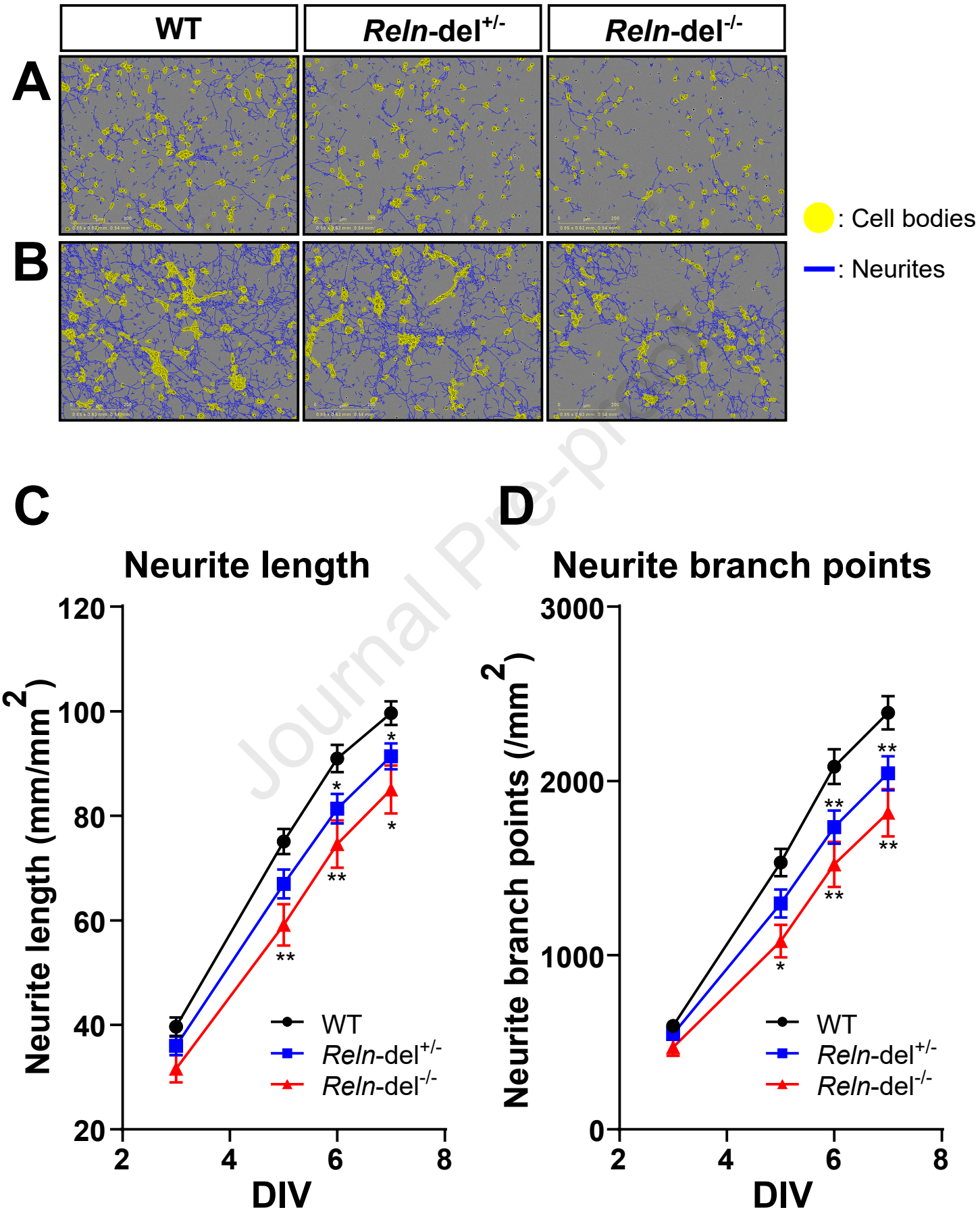

Figure 5 (E-F)

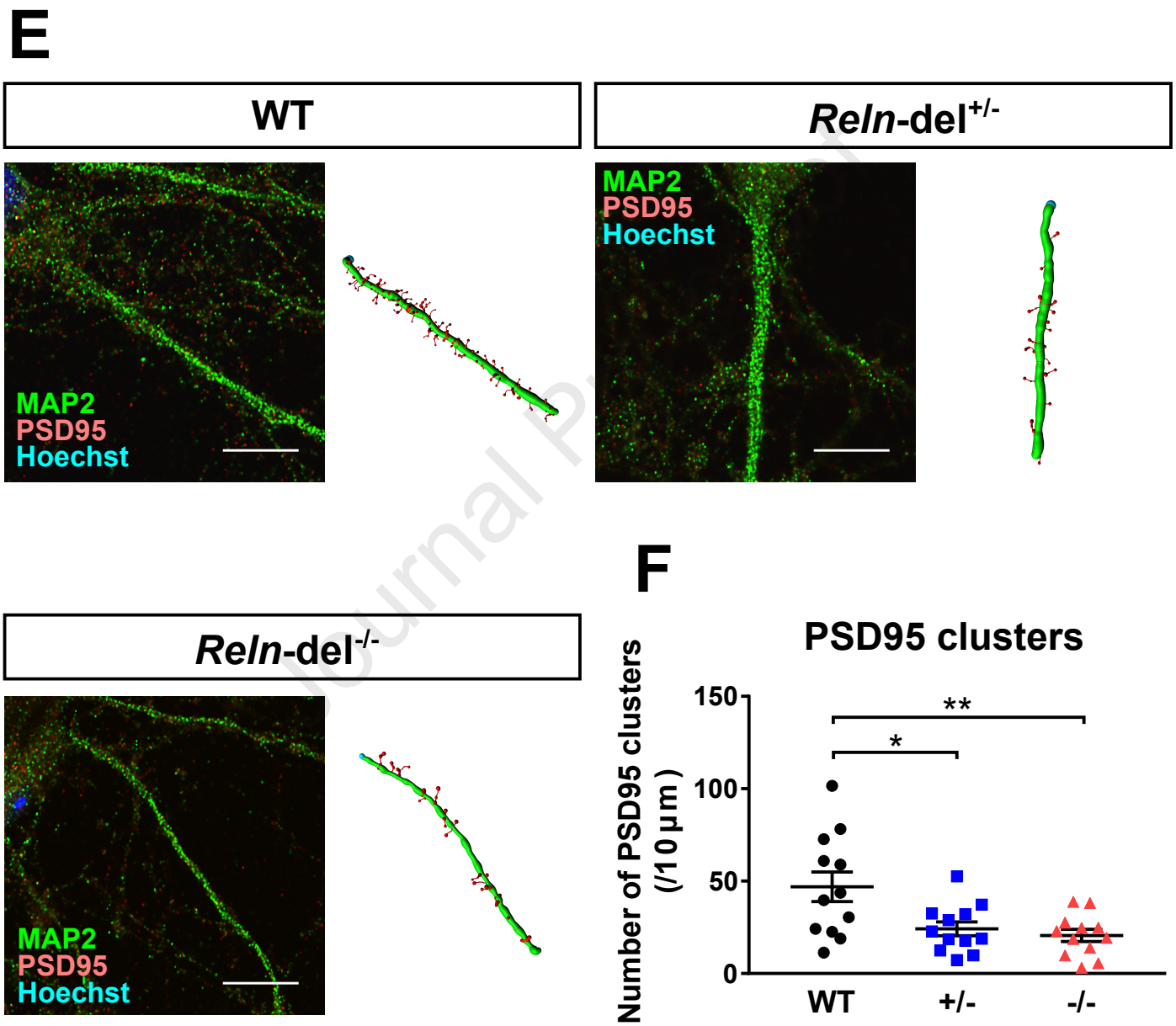

Figure 6

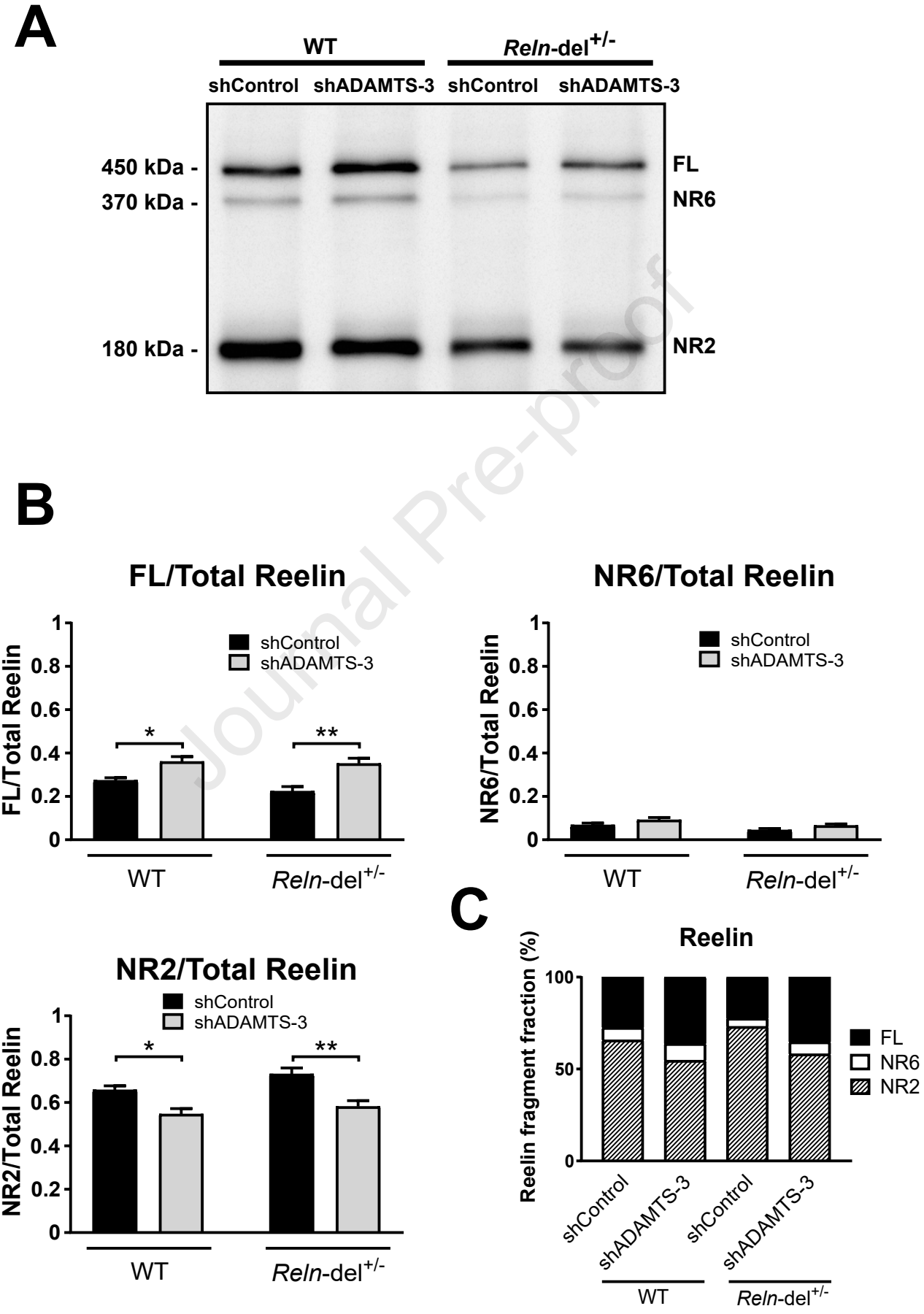

Figure 7

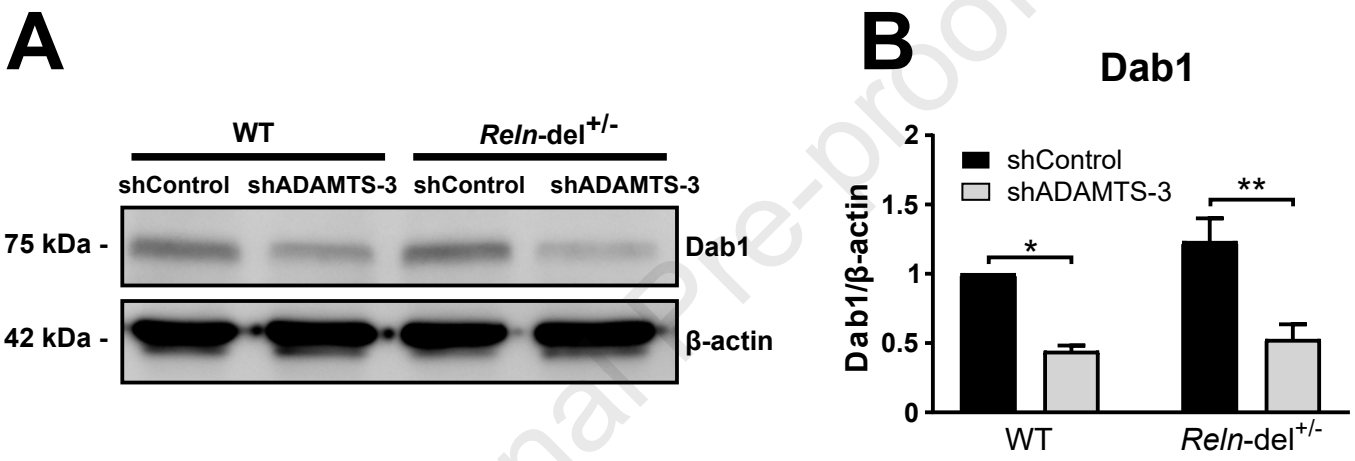

Highlights

• Reelin protein expression and secretion are decreased in *Reln*-del neurons.

• *Reln*-del neurons exhibit abnormal neurite development and spine formation.

• ADAMTS-3 knockdown may improve Reelin signaling by suppressing Reelin cleavage.

Declaration of competing interest

None.